

Article

Inventories of Short-Lived Fission Gas Nuclides in Nuclear Reactors

Yu Wang, Jianzhu Cao, Feng Xie *  and Fu Li

Institute of Nuclear and New Energy Technology, Collaborative Innovation Center of Advanced Nuclear Energy Technology, Key Laboratory of Advanced Reactor Engineering and Safety of Ministry of Education, Tsinghua University, Beijing 100084, China

* Correspondence: fxie@tsinghua.edu.cn

Abstract: Taking inventories in reactor cores is critical for understanding their radioactive source terms and establishing the relationship between the activity concentration in the primary loop and the status of the reactor core's fuel. However, there is a niche in which a simple but accurate relationship between reactor conditions and nuclide inventories can reliably predict the fission gas nuclide activities of the reactor core in the primary loop. In this study, a simple and efficient model called "Inventories of a Point Reactor for Fission Gas Nuclides" (IPRFGN) was proposed to calculate and interpret such inventories, in which a 10 MW high-temperature gas-cooled experimental reactor (HTR-10) was used as the test case. The present study findings were consistent with those of a general point-depletion burnup code such as the KORIGEN code. Here, the relative error was <1%. Based on the application of the IPRFGN model in HTR-10, the results indicate that the proposed IPRFGN model has provided the relationship between the inventories of fission gas nuclides in the core and the reactor conditions in all types of nuclear fission reactors. In the future, the IPRFGN model will be used for calculating fission gas nuclide inventories in various reactors.

Keywords: fission gaseous nuclides; inventory; source term; burnup; reactor power



Citation: Wang, Y.; Cao, J.; Xie, F.; Li, F. Inventories of Short-Lived Fission Gas Nuclides in Nuclear Reactors. *Energies* **2023**, *16*, 2530. <https://doi.org/10.3390/en16062530>

Academic Editor: Dan Gabriel Cacuci

Received: 27 January 2023

Revised: 22 February 2023

Accepted: 2 March 2023

Published: 7 March 2023



Copyright: © 2023 by the authors. Licensee MDPI, Basel, Switzerland. This article is an open access article distributed under the terms and conditions of the Creative Commons Attribution (CC BY) license (<https://creativecommons.org/licenses/by/4.0/>).

1. Introduction

Fission gas nuclides, including the radioisotopes Kr and Xe, are gaseous products of the nuclear fission reaction of fissile material. Fission gas nuclides are important considerations in the design of radiation monitoring systems and the implementation of radiation protection procedures in nuclear reactors as significant source terms in the primary loop [1–4], as these are also reflections of the operation conditions of fuel elements in a reactor core [5,6]. For example, radioactivity measurements are required for accurate monitoring of the damage of tri-structural isotropic (TRISO)-coated particles in the fuel elements of pebble-bed high-temperature gas-cooled reactors (HTGRs), where the fuel pebbles move in the core [6,7]. Fission gas nuclides in the reactor core and primary coolant are also the main sources of radioactive nuclides released into reactor buildings through leakages and the environment via discharges from the stack or relief valve during depressurization accidents [8,9]. Hence, inventories are required to evaluate and ensure reactor radiation safety.

Although nuclides such as ^{129}I , ^{131}I and ^{137}Cs exist, the main fission gas nuclides with a dominant contribution to the total activity in the primary coolant consist of $^{85\text{m}}\text{Kr}$, ^{87}Kr , ^{88}Kr , ^{89}Kr , ^{133}Xe , $^{133\text{m}}\text{Xe}$, ^{135}Xe , $^{135\text{m}}\text{Xe}$, ^{137}Xe , and ^{138}Xe regardless of the reactor type [10–12]. For instance, the activity fractions in various nuclear reactors such as M310, AP1000, the 10 MW high-temperature gas-cooled experimental reactor (HTR-10), and HTR-PM in normal operation conditions are approximately 81.90, 93.56, 69.77, and 84.06%, respectively [11], based on numerous online and offline radiation monitoring instruments that have been developed in the past to detect fuel elemental failures [13,14].

Inventories of fission gas nuclides are essential for quantifying the radioactive source terms and establishing the relationship between the activity concentration in the primary loop and the status of the fuel elements in the reactor core [15–17]. Reliable core inventories are also the basis for source term calculations, radiation protection, and accident analysis. Thus, accurately and efficiently calculating these inventories has been a relevant research area for the past several decades [18–21]. In addition, inventory calculations of radionuclides, including fission, fission metallic, and activation nuclides in various reactors are based on point depletion burnup equations, in which full-core calculations are divided into two steps: (1) determination of the point reactor equivalence model for a real reactor and (2) calculation of the solution for point depletion based on numerous inter-coupled ordinary differential equations (ODEs) [22–25].

Considering the neutron transport module in the core is necessary to determine the point reactor equivalence model for a real reactor, two approaches are applied for the coupling of neutron transport and depletion modules: the first approach involves solving the neutron transport equation using either deterministic or stochastic methods, in which the coupling is divided into deterministic neutron transport module depletion and stochastic neutron transport module depletion modules; the second approach involves simultaneously solving the neutron transport and point depletion equations using identified parameters, in which the equations can be classified into deep and shallow coupling modes [26]. Table 1 summarizes the computer codes of the main point depletion burnup for nuclide inventory calculations based on related studies from various countries. This demonstrates that burnup algorithms can be divided into two categories: analytic and numerical methods [27], which have been verified and validated in several recent studies. For example, Li et al. (2021) [28] alleviated the testing oracle problem using metamorphic techniques for the NUIT code, while Ilas and Hiscox (2021) [29] validated ORIGEN-S integrated into SCALE 6.2.4 and ENDF/B-VII.1 data libraries to analyze the nuclide inventory in pressurized water reactors (PWRs). Alves et al. (2020) [25] calculated the inventories of fission products and source terms to simulate the Argonaut nuclear reactor inside a severe accident using ORIGEN-2. Zwermann et al. (2021) [30] also provided discussions on the propagation of nuclear data uncertainties to decay heat and nuclide density using DARWIN/PEPIN2, while Castagna and Gilad (2022) [31] investigated the radionuclide inventory in nuclear fuel under uncertainties in boron concentrations using high-fidelity models. As for HTGRs, Cui et al. [32] researched uncertainty propagation of fission product yields from uranium and plutonium using pebble-bed burnup calculations. These point depletion burnup computer codes require detailed reactor physics calculations, which are based on the reactor and fuel designs, burnup-dependent fuel composition, locations of specific fuel assemblies in the core, and operational data from the reactor, in which numerous input parameters are normally needed; hence, these often do not meet rapid core diagnosis requirements for radiation monitoring of the primary coolant. To date, only a few studies have focused on the factors that affect inventories of fission gases in the nuclear reactor core.

Table 1. Point depletion burnup computer codes for nuclide inventory calculation.

Country	Code Name	Burnup Algorithms	References
Russia	AFPA	Transmutation trajectory analysis	[33]
Sweden	INVENT	(TTA) Method	[34]
Spain	ACAB	Matrix exponential methods	[35]
	FISP6	TTA	-
U.K.	FISPIN	Exponential Euler difference	[36]
	FISPACT	method	[37]
	DRAWIN-PEPIN	TTA	[38]
France	MECCYCO	A numerical method	[39]

Table 1. Cont.

Country	Code Name	Burnup Algorithms	References
Japan	DCHAIN	TTA	[40]
	CINDER		[41]
U.S.A.	ORIGEN	Matrix exponential methods	[42]
	ORIGEN-2		[43]
	ORIGEN-S		[44]
Germany	KORIGEN	Matrix exponential methods	[45]
	STACY-TNT		[46]
China	FLY	TTA/matrix exponential methods	[47]
	DEPTH		[48]
	NUIT		[49]
	GNIAC		[50]

To understand the features of the production chain of short-lived fission gases in the core and establish the relationship between their inventories and reactor parameters, this study aims to investigate the factors affecting the inventories of fission gas nuclides in reactors using a simple, novel, and efficient model called the “Inventories of a Point Reactor for Fission Gas Nuclides” (IPRFGN) to calculate the inventories of short-lived fission gas nuclides based on an analytical approach (Figure 1). In this study, only two reactor operational parameters (the reduced reactor power in the final stage, or the reactor power, and the average burnup of fuel elements, or the burnup) were used, in which all complex inputs in the point depletion burnup computer codes were reduced to 15 characteristic parameters for various specific reactors.

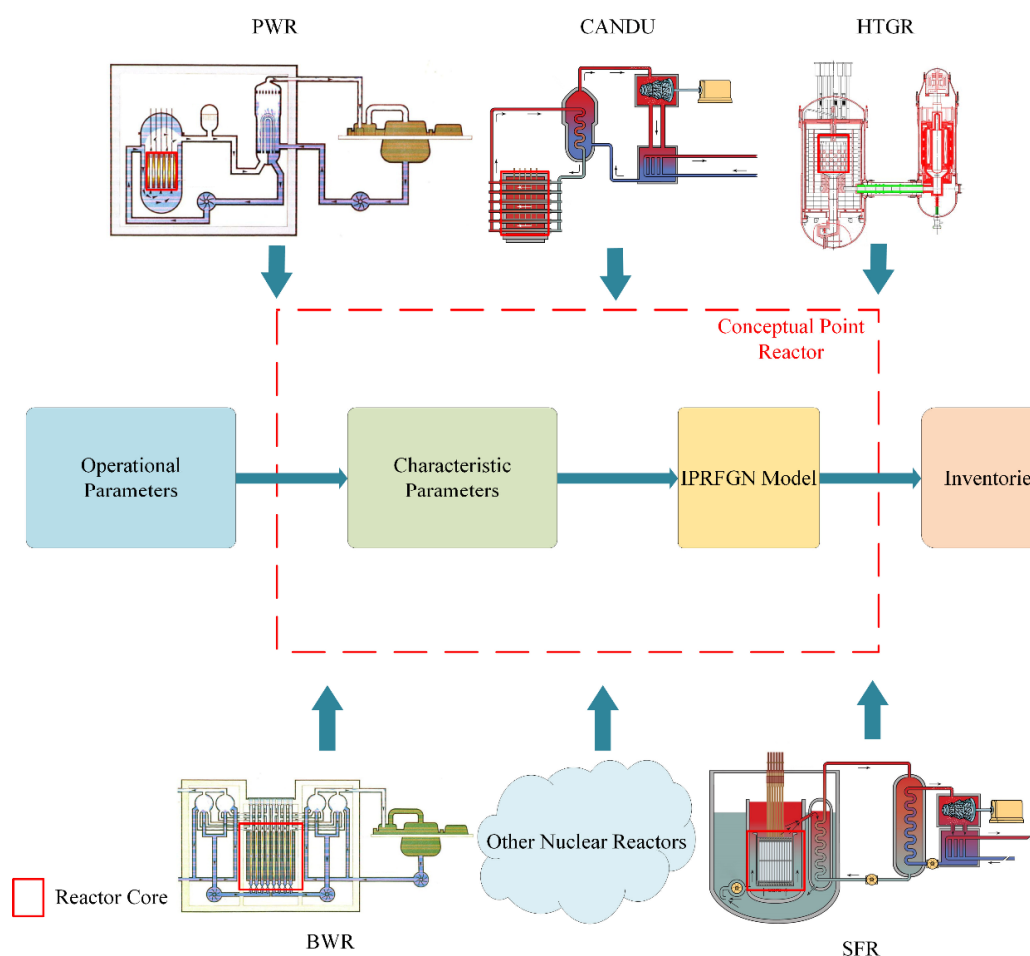


Figure 1. Schematic of the IPRFGN model [51,52].

To grasp the features of the production chain of short-lived fission gases in the core and establish the relationship between their inventories and reactor parameters will be significant for rapid core diagnosis in nuclear safety and nuclear emergency. This study elucidates, in detail, the factors affecting the inventories of fission gas nuclides in reactors. As shown in Figure 1, the present study proposes a simple, novel, and efficient model called the “Inventories of a Point Reactor for Fission Gas Nuclides” (IPRFGN) to calculate the inventories of short-lived fission gas nuclides for various types of nuclear reactors in an analytic form. Only two reactor operational parameters, which are the reduced reactor power in the final stage (denoted as reactor power) and the average burnup of fuel elements (denoted as burnup), are needed for the calculation of the inventories of short-lived fission gas nuclides for various types of nuclear reactors. All complex inputs in point depletion burnup computer codes are reduced into 15 characteristic parameters for several specific reactors.

To illustrate the model and calculate the inventories of various fission gas nuclides, HTR-10 is considered as an example. HTR-10 was built in Beijing, China, in 2000 and is the only pebble-bed type HTGR that can operate at full power in the world currently. The research on HTR-10 is of great importance for the development of HTGRs [7]. Further, the model is validated using the HTR-10 reactor as an example. The variations in typical fission gas nuclide inventories concerning reactor power and burnup are explained. The current model provides a clear and intuitive physical understanding of the relationship between the operating conditions of a reactor and the inventories of fission gas nuclides, which is useful for monitoring fuel elements in HTGRs and other nuclear fission reactors [13,14,53].

The remaining sections of the paper are organized as follows: The theoretical model and computational method, including the point depletion burnup equation and IPRFGN model, are presented in Section 2. Sections 3 and 4 comprise the results and discussion based on the HTR-10 calculation.

2. Method and Model

As previously stated, inventory calculations of radionuclides, including fission, fission metallic, and activation nuclides in various reactors are based on point depletion burnup equations, which can be divided into two steps: (1) determination of the point reactor equivalence model for a real reactor and (2) calculation of the solution for point depletion based on numerous inter-coupled ordinary differential equations (ODEs). This section focuses on Step (2) and introduces general point depletion equations and the IPRFGN model as a simplification of the former due to the properties of fission gas nuclides. Furthermore, computer codes for corresponding methods, KORIGEN and IPRFGN, are presented.

2.1. Point Depletion Burnup Equation

A fundamental procedure in nuclide inventory calculation is numerically solving the point depletion burnup equation, which is approximated using a system of linear first-order differential equations with constant coefficients and has been applied to hundreds of complex burnup chains involving thousands of nuclides. The general point depletion burnup equation is as follows [44]:

$$\frac{dN_i}{dt} = \sum_{j=1}^{n_j} l_{ij} \lambda_j N_j + \phi \sum_{j=1}^N f_{ij} \sigma_j N_j - (\lambda_i + \phi \sigma_{a,i}) N_i, \quad i = 1, 2, \dots, N \quad (1)$$

where N_i represents the atom numbers of radionuclide i ; N_j is the amount of precursor nuclide j or fissionable nuclides j ; n_j is the total number of precursor nuclides i ; N is the number of fissionable nuclides; λ_i is the decay constant of radionuclide i (s^{-1}); $\sigma_{a,i}$ is the spectrally averaged neutron absorption cross-section (cm^2); σ_j is the spectrally averaged cross-section that yields the nuclide i (cm^2); l_{ij} is the fraction from radionuclide j decay into nuclide i ; f_{ij} is the fraction from nuclides j to radionuclide i , particularly the fission yields

from fissionable nuclides j to radionuclide i ; and ϕ is the neutron flux averaged by space and energy ($\text{cm}^{-2} \text{s}^{-1}$) [44,45].

Using Equation (1), the inventories of hundreds of radionuclides produced by nuclear fission and other successive reactions, such as decay and neutron absorption, can be calculated. In a simpler form, this equation can also be used to calculate the inventories of fission gas nuclides. The source term of fission gas nuclides, which can be assumed to be constant over a short time for fuel fission, is defined as S_2 . The value of S_2 depends on the neutron flux and amounts of ^{235}U (N_{U5}), ^{238}U (N_{U8}), ^{239}Pu (N_{Pu9}), and ^{241}Pu (N_{Pu1}) for uranium dioxide fuel elements. Furthermore, because their precursor atom decay constants are much lower than those of fission gas nuclides, the number of precursor atoms achieves equilibrium and remains constant. Thus, the first term on the right side of Equation (1) can serve as a constant value, which is defined as S_1 . The burn-up equation for fission gas nuclide i can be approximated as follows:

$$\frac{dN_i}{dt} = -(\lambda_i + \phi\sigma_{a,i})N_i + S(N_j, \phi, N_{U5}, N_{U8}, N_{Pu9}, N_{Pu1}) \tag{2}$$

where S is a constant that is equal to $S_1 + S_2$.

The analytical solution can be easily derived by setting the initial atom N_i ($t = 0$) to 0 as follows:

$$I_i = \lambda_i N_i = \frac{\lambda_i S}{(\lambda_i + \phi\sigma_{a,i})} (1 - e^{-(\lambda_i + \phi\sigma_{a,i})t}) \tag{3}$$

where I_i is the activity inventory of nuclide i .

Owing to the large decay constant λ_i , fission gas nuclides can easily reach equilibrium, as shown in Equation (4):

$$I_i = \frac{\lambda_i S}{(\lambda_i + \phi\sigma_{a,i})} \tag{4}$$

Based on Equation (4), the equilibrium activity of the fission gas nuclide i is dependent on the neutron flux, decay constant, neutron absorption cross-section, all precursor nuclide equilibrium activities, and fissionable nuclides amounts, particularly ^{235}U , ^{238}U , ^{239}Pu , and ^{241}Pu .

2.2. IPRFGN Model

The IPRFGN model, which describes the various reactor cores as a point reactor characterized by several key parameters, was used to effectively calculate the inventories of fission gas nuclides in the point reactor. As shown in Figure 2, the calculation flow illustrates the processes, in which they are connected by dashed lines following the types of reactor, including the different enrichment levels of uranium and plutonium in the fuel elements. Here, the calculated inventories in similar enrichment levels and types of reactor depend on the given operational parameters such as the reactor power and burnup.

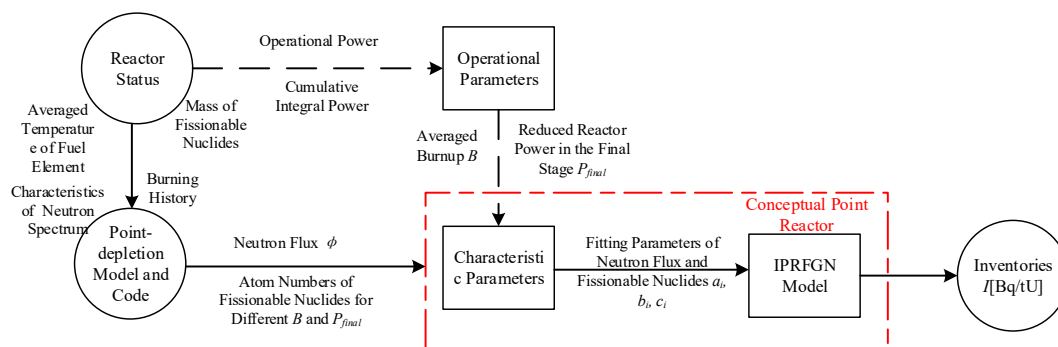


Figure 2. Calculation flow of the IPRFGN model.

Fission gas nuclides normally have two general modes in terms of the number of decay chains: General Modes A and B. In this study, both modes were evaluated. The former is depicted in Figure 3a [45,54], in which the reaction branching ratios were obtained from KORIGEN nuclear data libraries, as these were the most recent data available from the Evaluated Nuclear Structure Data File (ENSDF) of the International Atomic Energy Agency (IAEA) [45,55,56].

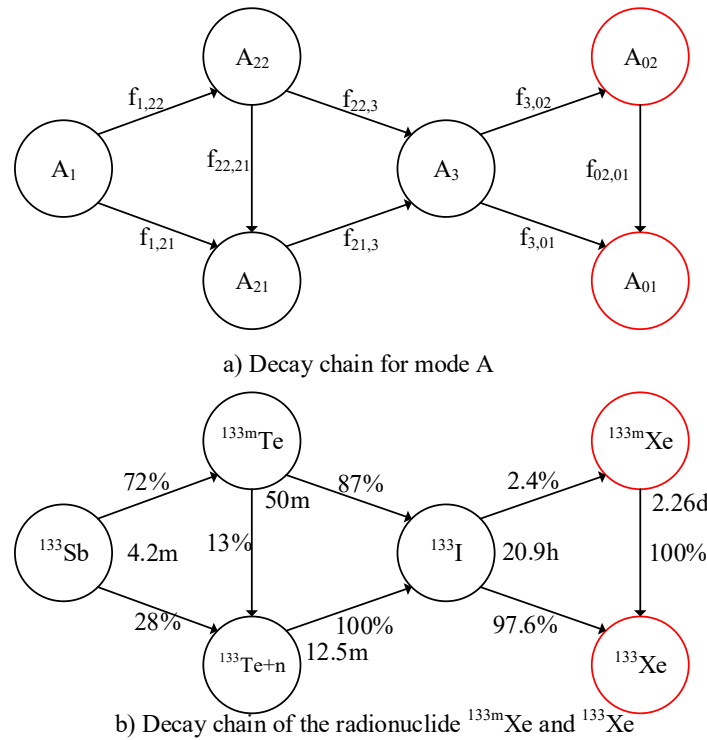


Figure 3. General Mode A for the decay chain.

Further, General Mode A was derived from the decay chain for ^{133}Xe and ^{133m}Xe in Figure 3b, in which the 100% decay fraction was omitted for simplification. In Figure 3, A_i refers to the activity of nuclide i , where i can be equal to 1, 21, 22, 3, 01, or 02; and $f_{i,j}$ refers to the decay fraction from nuclide i to nuclide j .

Equations (5)–(10) are the point depletion burnup equations for General Mode A, where $\sum_j f_{i,j} = 1, j = 1 \dots n_j$. $A_{f,i}$ is defined as the source of nuclide i obtained directly from fissionable fuel nuclides (atoms):

$$\frac{dN_{01}}{dt} = -(\lambda_{01} + \sigma_{a,01}\phi)N_{01} + (f_{02,01}\lambda_{02}N_{02} + f_{3,01}\lambda_3N_3) + A_{f,01} \tag{5}$$

$$\frac{dN_{02}}{dt} = -\lambda_{02}N_{02} + f_{3,02}\lambda_3N_3 + A_{f,02} \tag{6}$$

$$\frac{dN_3}{dt} = -\lambda_3N_3 + f_{21,3}\lambda_{21}N_{21} + f_{22,3}\lambda_{22}N_{22} + A_{f,3} \tag{7}$$

$$\frac{dN_{21}}{dt} = -\lambda_{21}N_{21} + f_{1,21}\lambda_1N_1 + f_{22,21}\lambda_{22}N_{22} + A_{f,21} \tag{8}$$

$$\frac{dN_{22}}{dt} = -\lambda_{22}N_{22} + f_{1,22}\lambda_1N_1 + A_{f,22} \tag{9}$$

$$\frac{dN_1}{dt} = -\lambda_1N_1 + A_{f,1} \tag{10}$$

The following conditions were applied for the above equations:

- The (n, γ) neutron absorption reaction was only considered for ^{135}Xe and ^{133}Xe ;

- ^{235}U , ^{238}U , ^{239}Pu , and ^{241}Pu were considered for fissionable nuclides;
- All fission gas nuclides were assumed to be in equilibrium, where $\frac{dN_i}{dt} = 0$, $i = 1, 21, 22, 3, 01, \text{ or } 02$.

For the second characteristic, $A_{f,j}$ can be written as follows:

$$A_{f,j} = \sum_i Y_{i,j} \sigma_{f,i} \phi N_i \quad i = U5, U8, Pu9, Pu1 \tag{11}$$

where $\sigma_{f,U5}$, $\sigma_{f,U8}$, $\sigma_{f,Pu9}$, and $\sigma_{f,Pu1}$ are the fission cross-sections of ^{235}U , ^{238}U , ^{239}Pu , and ^{241}Pu , respectively (cm^2); and $Y_{U5,j}$, $Y_{U8,j}$, $Y_{Pu9,j}$, and $Y_{Pu1,j}$ are fission yields of nuclide j from fissionable nuclides ^{235}U , ^{238}U , ^{239}Pu , and ^{241}Pu , respectively. All fission yields and cross sections were obtained from the nuclear data libraries of KORIGEN. Three-group pre-generated nuclear data were calculated by Karlsruhe Institute of Technology (KIT) using Evaluated Nuclear Data File (ENDF) in the IAEA database. The characteristic neutron flux spectrum was supplied for four types of nuclear reactors: HTGR, light water reactor (LWR), liquid metal fast breeder reactor (LMFBR), and molten salt breeder reactor (MSBR) [33,43]. Further inspection of Equation (11) reveals that $A_{f,j}$ was proportional to the neutron flux ϕ .

The analytical results are listed below:

$$I_{02} = \lambda_{02} N_{02} = f_{3,02} (A_{f,1} + A_{f,21} + A_{f,22} + A_{f,3}) + A_{f,02} \tag{12}$$

$$I_{01} = \lambda_{01} N_{01} = (A_{f,1} + A_{f,21} + A_{f,22} + A_{f,3} + A_{f,02} + A_{f,01}) \frac{\lambda_{01}}{\lambda_{01} + \sigma_{a,01} \phi} \tag{13}$$

where I_i is the inventory of nuclide i (Bq).

General Mode A includes four sub-modes with the same or simpler forms, and A_0 , A_1 , A_2 , and A_3 were used as their representation, including three other sub-modes, as shown in Figure 4. Meanwhile, General Mode B was derived from the decay chain of ^{88}Kr , as shown in Figure 5b.

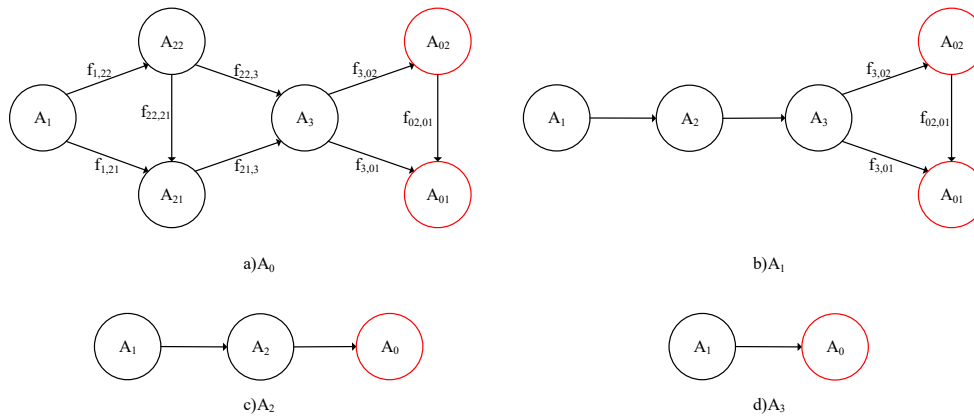


Figure 4. Sub-modes of General Mode A for the decay chain of the fission gas nuclide.

Hence, the equilibrium inventory of the fission gas nuclide i (I_i) can be obtained from the linear combination of the source of nuclide j in the entire decay chain of nuclide i ($A_{f,j}$) and can be expressed as Equation (14). Additional details are provided in Table 2. All justification of equations is discussed in the supporting information.

$$I_i = g(A_{f,j}) = \sum_j \alpha_{j,i} A_{f,j} \tag{14}$$

where $\alpha_{j,i}$ is the linear coefficient of the source of nuclide i obtained directly from fissionable fuel nuclides j .

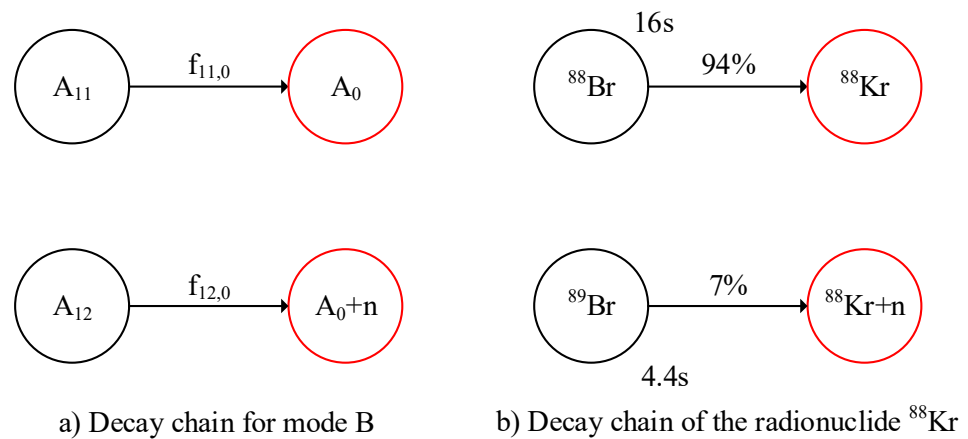


Figure 5. General Mode B for the decay chain.

Table 2. Classification and solutions of fission gas nuclides for general modes.

General Mode	Nuclide	Solutions
A_0	$^{133}\text{Xe}, ^{133\text{m}}\text{Xe}$	$I_{01} = (A_{f,1} + A_{f,21} + A_{f,22} + A_{f,3} + A_{f,02} + A_{f,01}) \frac{\lambda_{01}}{\lambda_{01} + \sigma_{a,01}\phi}$ $I_{02} = f_{3,02} (A_{f,1} + A_{f,21} + A_{f,22} + A_{f,3}) + A_{f,02}$
A_1	$^{135}\text{Xe}, ^{135\text{m}}\text{Xe}$	$I_{01} = (A_{f,1} + A_{f,2} + A_{f,3} + A_{f,02} + A_{f,01}) \frac{\lambda_{01}}{\lambda_{01} + \sigma_{a,01}\phi}$ $I_{02} = f_{3,02} (A_{f,1} + A_{f,2} + A_{f,3}) + A_{f,02}$
A_2	$^{85\text{m}}\text{Kr}$	$I_0 = f_{2,0} (f_{1,2} A_{f,1} + A_{f,2}) + A_{f,0}$
A_3	^{89}Kr	$I_0 = f_{1,0} A_{f,1} + A_{f,0}$
B	^{87}Kr	$I_0 = f_{11,0} A_{f,11} + f_{12,0} A_{f,12} + A_{f,0}$
	^{88}Kr	
	^{137}Xe	

2.3. KORIGEN and IPRFGN

Based on the ORIGEN code created by Oak Ridge National Laboratory (ORNL), the KORIGEN code was developed to calculate isotope generation and depletion and was modified by the Institute for Neutron Physics and Reactor Technology (INR) at the KIT [45]. The KORIGEN code was used in this study to evaluate the nuclide inventories and depletion and burnup of nuclear fuels loaded into the reactor core, in which the neutron reaction rates of each burnup step were evaluated, and the radioactivity inventories of various reactors were evaluated regardless of the in-pile fuel or spent fuel.

The WrapKORIGEN code, developed by the Institute of Nuclear and New Energy Technology (INET) at Tsinghua University, refers to a series of Python scripts that were used in the pre- and post-processing of the KORIGEN-based inventory calculations for the full-core reactor; it was also used to examine the factors that can affect radionuclide inventories in this study.

Similarly, the IPRFGN code, which was similarly developed by the INET, focuses on the inventories of equilibrium and non-equilibrium conceptual reactors. The IPRFGN model was described above using an analytical approach.

3. Results

3.1. Conceptual Point Reactor for the Equilibrium Core of HTR-10

In this study, the conceptual point reactor was used as an idealized physical model to calculate the inventories of fission gas nuclides, in which a series of parameters were

adopted to represent a specific reactor and determine core inventory calculations. Specifically, the neutron flux and atom numbers ^{235}U , ^{238}U , ^{239}Pu , and ^{241}Pu were assigned as the characteristic parameters. However, the effect of ^{241}Pu can be neglected as pure uranium dioxide fuel elements were used in HTR-10. In the current conceptual point reactor, four parameters in the form of a quadratic function were adopted as follows:

$$\phi = (a_{\phi}B^2 + b_{\phi}B + c_{\phi}) \cdot \frac{P_{final}}{74.6} \quad (15)$$

$$N_i = (a_iB^2 + b_iB + c_i), \quad i = \text{U5}, \text{U8}, \text{ and Pu9} \quad (16)$$

where a , b , and c are parameters of the conceptual point reactor, P_{final} is the reactor power (MW/tU), and B is the burnup (GWd/tU).

The various types of reactors and their corresponding reactor type with various loaded fuels were found to have divergencies. In Table 3, the conceptual point reactor for HTR-10 at equilibrium is presented. Accordingly, these were fitted with the result of the point depletion burnup computer code KORIGEN. Here, the inventories of short-lived fission gas nuclides for an individual reactor with specific loaded fuel were found to be dependent on two operational parameters: the reactor power and burnup in our conceptual point reactor.

Table 3. Parameters of the conceptual point reactor for the equilibrium core of HTR-10.

	ϕ	N_{U5}	N_{U8}	N_{Pu9}
a	8.45×10^8	5.86×10^{21}	-3.54×10^{21}	-8.11×10^{20}
b	2.49×10^{10}	-3.15×10^{24}	-6.00×10^{23}	2.11×10^{23}
c	2.11×10^{13}	4.36×10^{26}	2.10×10^{27}	7.04×10^{24}

The findings revealed that the obtained full-core reactor values were relatively close to the average conceptual point reactor. In real engineering design and operation, the conceptual point reactor can reliably and effectively substitute the full-core reactor. Hence, the results obtained in this study can similarly be substituted for full-core reactor values, in which the observed physical characteristics were noted in the equilibrium core of HTR-10. The KORIGEN code was used as a reference.

3.2. Neutron Flux

As the reduced reactor power in the final stage refers to the operational power of the reactor per ton of fissionable material (MW/tU) before the experiment duration, the operating history was not relevant. Meanwhile, the average burnup of fuel elements refers to the amount of energy extracted per mass of the initial loaded fuel. In addition, it is given by megawatt-days per metric ton of heavy metal loaded (MWd/MTHM); however, the unit adopted in this study was gigawatt-days per metric ton of uranium (GWd/tU).

In Figure 6, the neutron flux derived from the KORIGEN code for the equilibrium core of HTR-10 was shown to increase with an increase in the reactor power and burnup. The proportional relationship between the neutron flux and reactor power is due to the proportional relationship between the reactor power and the number of nuclear fission reactions per unit of time, as well as the proportional relationship between the neutron flux and the number of nuclear fission reactions per unit of time. Regarding the increase in neutron flux as burnup increases, the neutron flux rises to compensate for the consumption of total fissile material to maintain constant reactor power as burnup increases.

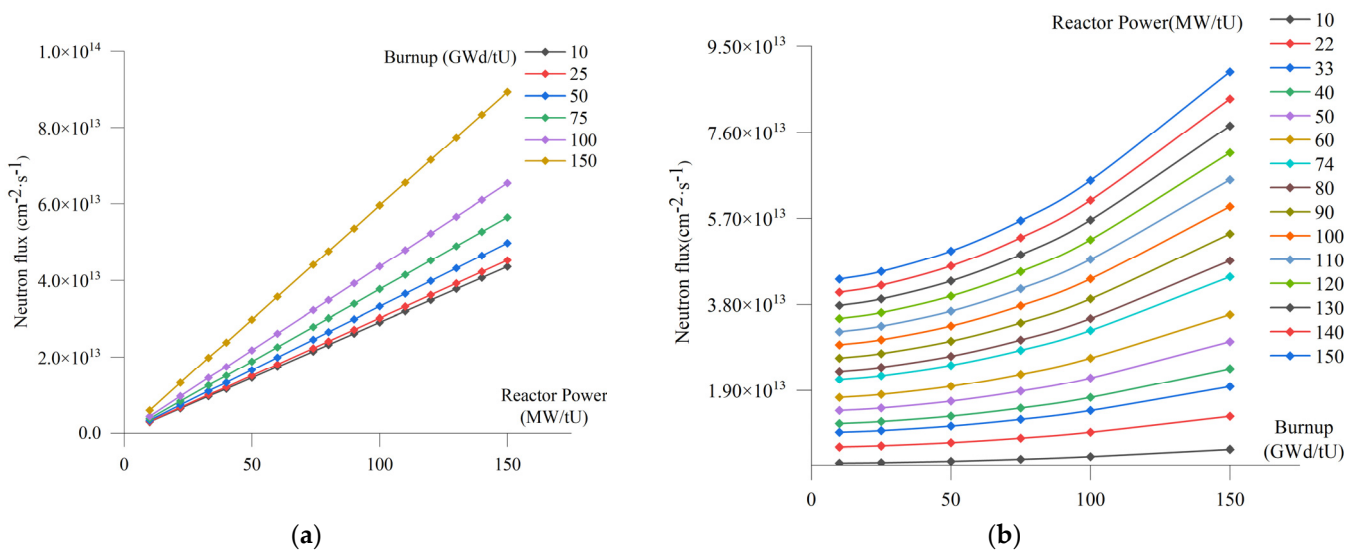


Figure 6. Relationships between the neutron flux and (a) reactor power and (b) burnup.

It also fitted with the quadratic function of burnup with a fixed reactor power, which can be defined as a function of the reactor power and burnup:

$$\phi = \phi_{ref} \frac{P_{final}}{P_{ref}} \tag{17}$$

where ϕ_{ref} is the reference neutron flux at the reference reactor power (P_{ref} , 74.6 MW/tU). ϕ_{ref} was fitted as a quadratic function using least-squares fitting:

$$\phi_{ref} \approx 8.45 \times 10^8 B^2 + 2.49 \times 10^{10} B + 2.11 \times 10^{13} \tag{18}$$

$$\phi = \phi(B, P_{final}) = \left(8.45 \times 10^8 B^2 + 2.49 \times 10^{10} B + 2.11 \times 10^{13} \right) \cdot \frac{P_{final}}{74.6} \tag{19}$$

In Table 4, the neutron flux values derived from Equation (19) were compared with those calculated using the KORIGEN code with an obtained burnup value and reactor power of 10–150 GWd/tU and 10–150 MW/tU, respectively. It was found that the values were relatively consistent, with relative errors of <1.0%. Hence, this demonstrates that the neutron flux is determined by fitting Equation (19) with the results from the KORIGEN code.

Table 4. Variance between current results from Equation (19) and those from KORIGEN.

P_{final} (MW/tU)	B (GWd/tU)					
	10	25	50	75	100	150
10	−0.35%	0.00%	−0.36%	−0.55%	−0.39%	−0.69%
22.22	−0.26%	0.12%	−0.40%	−0.59%	−0.33%	−0.20%
33.33	−0.26%	0.32%	−0.66%	−0.83%	−0.40%	−0.20%
40	−0.01%	0.33%	−0.50%	−0.68%	−0.39%	−0.36%
50	−0.01%	0.33%	−0.36%	−0.29%	−0.16%	−0.19%
60	−0.01%	0.33%	−0.25%	−0.02%	−0.01%	−0.08%
74	−0.20%	0.33%	−0.08%	−0.20%	0.20%	−0.06%
80	−0.01%	0.33%	−0.13%	−0.02%	0.18%	0.06%
90	−0.01%	0.33%	0.25%	0.13%	0.25%	0.30%
100	−0.35%	0.33%	−0.05%	−0.02%	0.30%	0.32%
110	−0.01%	0.64%	0.25%	0.10%	0.55%	0.49%

Table 4. Cont.

P_{final} (MW/tU)	B (GWd/tU)					
	10	25	50	75	100	150
120	−0.01%	0.61%	0.25%	0.20%	0.57%	0.63%
130	−0.01%	0.59%	0.48%	0.29%	0.76%	0.62%
140	−0.01%	0.81%	0.47%	0.36%	0.76%	0.73%
150	−0.01%	0.78%	0.45%	0.60%	0.92%	0.83%

3.3. Fissionable Nuclides

The calculated results for the full-core inventory of the HTR-10 fueled by low-enriched uranium (LEU) indicated that most fission products were obtained from three main fissionable isotopes, namely, ^{235}U , ^{238}U , and ^{239}Pu . The initial fraction of ^{235}U in the uranium was 17%. Based on the calculations in this study, the number of atoms of ^{235}U and ^{238}U decrease from 4.05×10^{26} and 2.10×10^{27} to 9.46×10^{25} and 1.93×10^{27} , respectively. In contrast, the number of ^{239}Pu atoms increased from 9.08×10^{24} to 2.05×10^{25} .

Mills et al. (2020) [57] proposed a method for estimating the fractional fission rates of major nuclides in light water and advanced gas-cooled reactors in terms of anti-neutrino emission, particularly when a reactor is at constant power. Here, a series of simplified equations with several key parameters were selected to describe the fractional fission rates of major nuclides by ignoring irrelevant parameters. This series was closely related to the neutron flux and the number of major fissionable atoms in the nuclear reactor. Hence, a similar simplification approach was used in the present study.

Based on the relationship between the fractional fission and the number of fissionable atoms, including the few effects of ^{241}Pu on the inventory calculation of HTR-10, the following equations are proposed to evaluate the number of major atoms (^{235}U , ^{238}U , and ^{239}Pu) using the least-squares fitting method:

$$N_{U5} = 5.86 \times 10^{21} B^2 - 3.15 \times 10^{24} B + 4.36 \times 10^{26} \quad (20)$$

$$N_{U8} = -3.54 \times 10^{21} B^2 - 6.00 \times 10^{23} B + 2.10 \times 10^{27} \quad (21)$$

$$N_{Pu9} = -8.11 \times 10^{20} B^2 + 2.11 \times 10^{23} B + 7.04 \times 10^{24} \quad (22)$$

Figure 7 depicts that the number of atoms of ^{235}U and ^{238}U are significantly larger than those of ^{239}Pu . However, the number of ^{239}Pu atoms was only comparable with that of ^{235}U in the same order of magnitude, given that the burnup value exceeded ~ 100 GWd/tU.

Figure 8 shows that the variations in the number of fissionable atoms were associated with an increase in the burnup value. These variations differed significantly for major nuclides, where relevant atom number variations take the number of fissionable atoms, with a burnup value of 10 GWd/tU used as a reference. These variations were obtained by subtracting the number of fissionable atoms in the initial fuel from those in the fuel with a higher burnup value from the number of fissionable atoms in the initial fuel. Changes in the number of ^{238}U atoms were relatively small, with a maximum value of -7.80% , whereas the relative variations of the number of atoms of ^{235}U and ^{239}Pu were significantly larger with a maximum value of -76.63 and 125.90% , respectively. The linearity of the curve of ^{238}U can also be attributed to the large value and small consumption of the number of atoms. Furthermore, the relative variation of the number of ^{239}Pu was observed to increase with the increase in burnup, until it gradually decreased, which can be attributed to the competition processes between the neutron fission reaction of ^{239}Pu and activation of ^{238}U to ^{239}Pu , which vary with the increase in burnup.

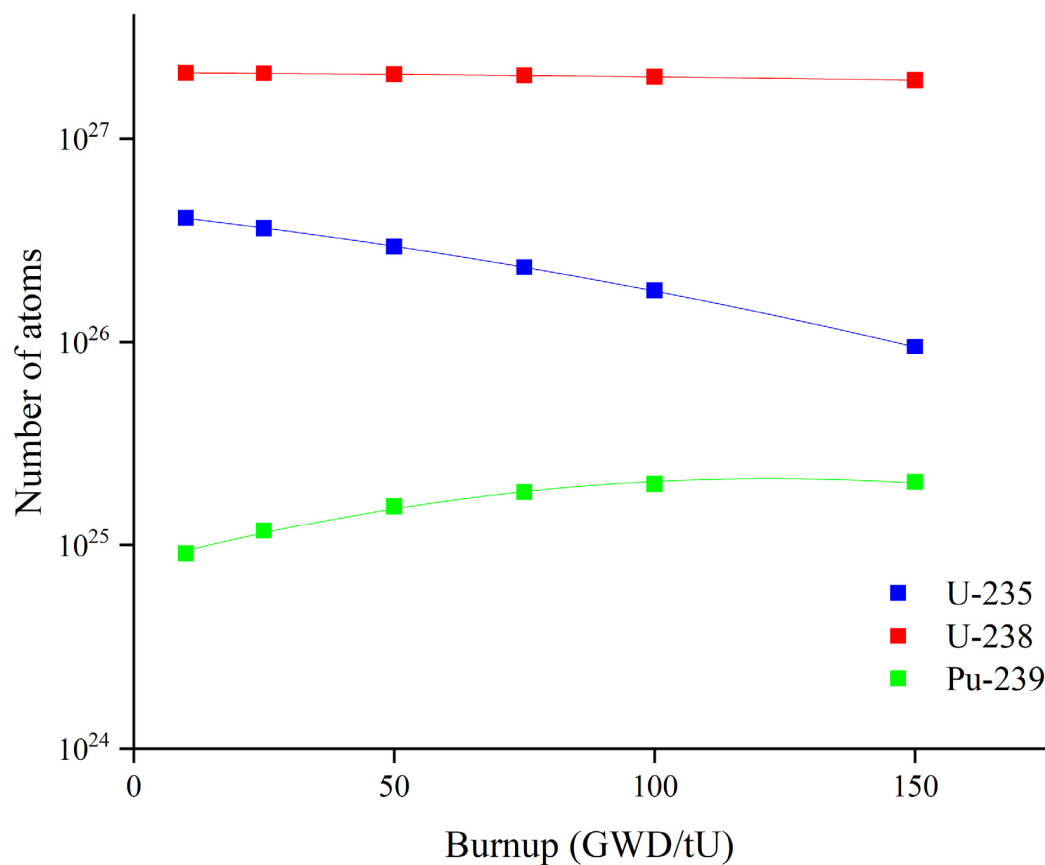


Figure 7. Number of fissionable atoms (²³⁵U, ²³⁸U, and ²³⁹Pu) versus burnup.

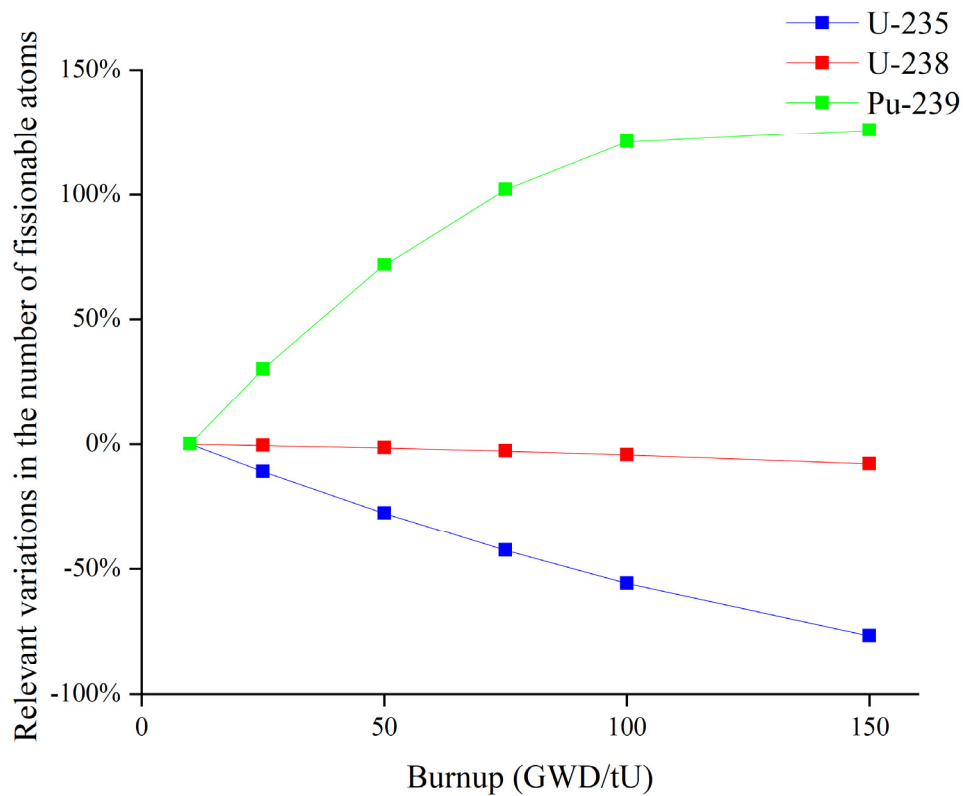


Figure 8. Relevant variations in the number of fissionable atoms (²³⁵U, ²³⁸U, and ²³⁹Pu).

3.4. Inventories of Short-Lived Fission Gas Nuclides

Figure 9 shows the plot of the two inventories at fixed burnup values of 10 and 100 GWd/tU, respectively. All inventories of the fission gas nuclides were distributed within the range of 10^{15} – 10^{18} Bq/tU in a descending order as follows: ^{133}Xe , ^{138}Xe , ^{137}Xe , ^{89}Kr , ^{88}Kr , ^{87}Kr , $^{85\text{m}}\text{Kr}$, $^{135\text{m}}\text{Xe}$, and $^{133\text{m}}\text{Xe}$. Particularly, ^{135}Xe exhibited distinct behaviors. Figure 9 depicts that the inventories of fission gas nuclides excluding ^{135}Xe , i.e., $^{85\text{m}}\text{Kr}$, ^{87}Kr , ^{88}Kr , ^{89}Kr , ^{133}Xe , $^{133\text{m}}\text{Xe}$, $^{135\text{m}}\text{Xe}$, ^{137}Xe , and ^{138}Xe , were proportional to the reactor power in the final stage. Notably, the inventory of ^{135}Xe increased proportionally to the reactor power, with a gradual decrease toward the equilibrium state ($\sim 7.94 \times 10^{16}$ Bq/tU).

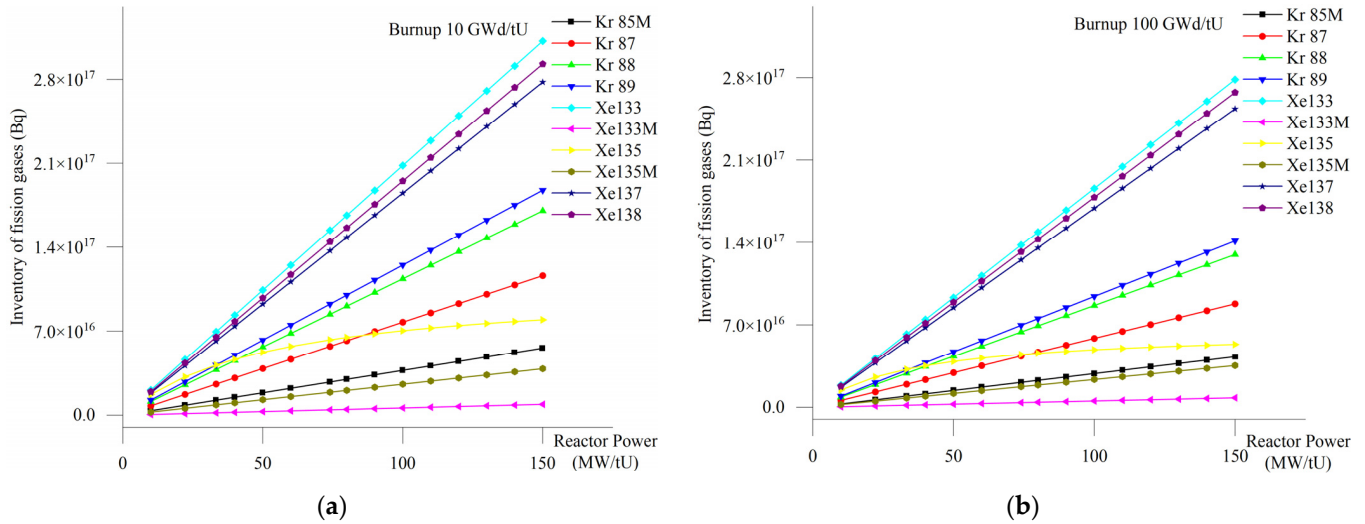


Figure 9. Inventories of fission gas nuclides with various reactor powers under fixed burnup: (a) 10 and (b) 100 GWd/tU.

Based on the general mode analysis and the determined relationship between the proportion of $A_{f,i}$ and the neutron flux (ϕ), only the ^{133}Xe and ^{135}Xe inventories were relevant to the neutron flux. The equilibrium inventory for the fission gas nuclide i (I_i) was also found to be a linear combination of the source of nuclide j in the entire decay chain of nuclide i ($A_{f,j}$), in which the reactor power was proportional to the neutron flux at the same fuel burnup value. Hence, the inventories of fission gas nuclides excluding ^{135}Xe , i.e., $^{85\text{m}}\text{Kr}$, ^{87}Kr , ^{88}Kr , ^{89}Kr , ^{133}Xe , $^{133\text{m}}\text{Xe}$, $^{135\text{m}}\text{Xe}$, ^{137}Xe , and ^{138}Xe , were all proportional to the reactor power.

The inventories of ^{133}Xe and ^{135}Xe can be expressed as follows:

$$I_{01} = A_f(\phi) \frac{\lambda_{01}}{\lambda_{01} + \sigma_{a,01}\phi} \quad (23)$$

where A_f is the whole source from each nuclide in the corresponding decay chains, in which it was proportional to the neutron flux ϕ . Given that the value of $\sigma_{a,01}\phi$ was comparable to λ_{01} , such as those in ^{135}Xe , the inventory of ^{135}Xe increases as the neutron flux increases; however, it was found to progress more gradually compared to other inventories as λ_{01} becomes more negligible as the neutron flux increases. A limit value also existed when ϕ approached infinity, as shown in Equation (24). For ^{133}Xe , ϕ did not approach infinity; thus, $\sigma_{a,01}$ was inferred to be inadequate, which makes $\sigma_{a,01}\phi$ incomparable with λ_{01} . Hence, this resulted in similar exhibited behaviors in the inventory of ^{133}Xe compared to those of other fission gas nuclides.

$$I_{01} = A_f(\phi) \frac{\lambda_{01}}{\sigma_{a,01}\phi} = A_f(\text{Constant}), \quad \sigma_{a,01}\phi \gg \lambda_{01} \quad (24)$$

As shown in Figure 10, for fixed reactor power, all inventories of fission gas nuclides decreased as the burnup value increased. Several isotopes, such as ^{133}Xe , $^{133\text{m}}\text{Xe}$, ^{137}Xe , and ^{138}Xe , were found to be more independent of the burnup in the lower burnup region. In contrast, all the inventories tended to have decreased proportional relationships, particularly in the higher burnup region.

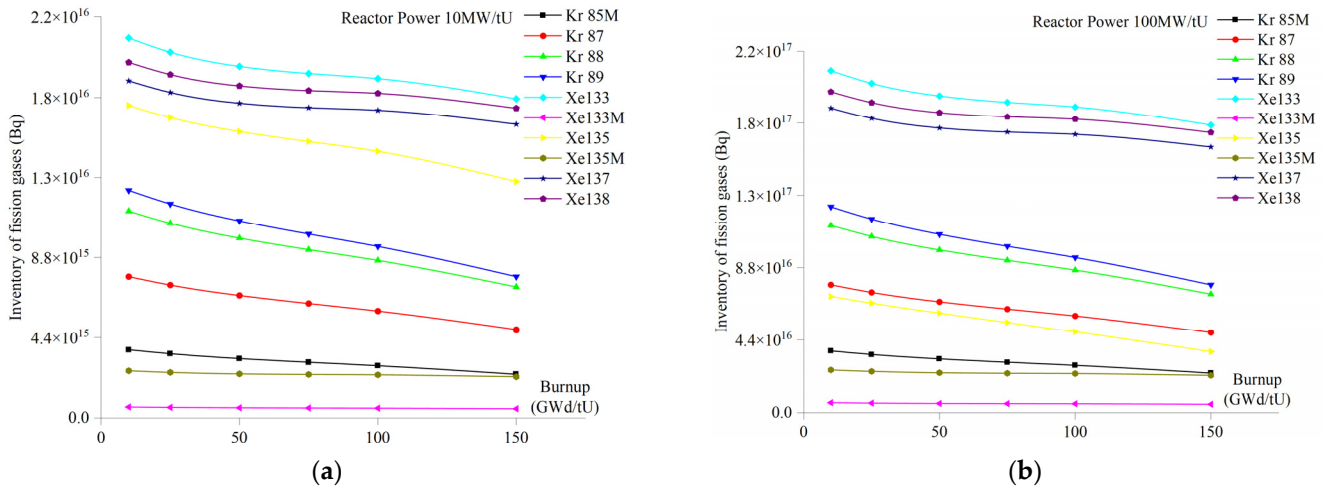


Figure 10. Inventories of fission gas nuclides with increasing burnup under fixed reactor power: (a) 10 and (b) 100 MW/tU.

Despite the simultaneous production of ^{239}Pu in the low burnup region, the main inventories of fissionable nuclides, including ^{238}U and ^{235}U , gradually decreased. The neutron flux increased as the burnup value increased for the same reactor power. These findings indicate that the consumption of fissionable nuclides ^{238}U and ^{235}U can be accounted as the main contribution. Therefore, the inventory of fission gas nuclide i can be recalculated as follows:

$$I_i = g(A_{f,j}) = \sum_j \alpha_{j,i} A_{f,j} = \sum_k \beta_{k,i}(\phi) N_k, \quad j, k = U5, U8, Pu9 \quad (25)$$

where $\beta_{k,i}$ is a linear coefficient for radionuclide i based on the number of fissionable atoms k , as shown in Equation (26):

$$\beta_{k,i} = \sum_j (\alpha_{j,i} Y_{k,j} \sigma_{f,k}) \phi \quad (26)$$

For the same nuclide i (except ^{135}Xe), the variables in $\beta_{k,i}$ were constant. The variation in I_i was derived from the divergences of ϕ , N_{U5} , N_{U8} , and N_{Pu9} , in which the sequence was: $N_{U8} \gg N_{U5} > N_{Pu9} \gg \phi$. Furthermore, with a similar increase in burnup value, ^{238}U showed the least variation, followed by ^{235}U and ^{239}Pu . Hence, it is inferred that a larger value of $\beta_{U8,i}$ corresponds to a more constant slope for the nuclide i (Figure 10). All nuclides in the decay chain defined as nuclide j will also be more dependent on the number of ^{238}U atoms. I_i can be approximated using Equation (27) in the higher burnup region, as follows:

$$I_i \approx \beta_{U8,i} N_{U8} \quad (27)$$

As previously mentioned, N_{U8} has sufficient linearity and thus explains the proportional decreases in the higher burnup region.

4. Discussion

4.1. Code-to-Code Comparison

Table 5 lists the relevant variations between the KORIGEN and IPRFGN codes for calculating $^{85\text{m}}\text{Kr}$, which were subsequently used to validate the proposed IPRFGN model.

As these variations were obtained from the differences between the results of both models, the variations in other fission gas nuclides all corresponded to <1% under a reactor power of 0–150 MW/tU and a burnup value of 0–150 GWd/tU, which was similar to the results obtained in ^{85m}Kr in Table 5.

Table 5. Code-to-code comparison with various reactor powers and burnups for ^{85m}Kr .

P_{final} (MW/tU)	B (GWd/tU)					
	10	25	50	75	100	150
10	0.14%	0.15%	−0.18%	0.10%	0.53%	−0.86%
22.22	0.18%	−0.02%	−0.02%	0.21%	0.38%	−0.47%
33.33	0.03%	0.14%	−0.19%	0.21%	0.38%	−0.71%
40	0.14%	0.20%	−0.12%	−0.02%	0.39%	−1.02%
50	0.04%	0.15%	−0.18%	−0.02%	0.53%	−0.70%
60	0.14%	0.11%	−0.22%	−0.02%	0.39%	−0.75%
74	0.04%	−0.07%	−0.31%	0.01%	0.41%	−0.84%
80	0.14%	0.07%	−0.26%	−0.02%	0.39%	−0.82%
90	0.08%	0.05%	−0.28%	−0.02%	0.47%	−0.84%
100	0.04%	0.03%	−0.30%	0.08%	0.36%	−0.92%
110	−0.36%	0.41%	−0.30%	−0.02%	0.45%	−0.87%
120	−0.36%	−0.07%	−0.59%	−0.02%	0.39%	−0.88%
130	0.41%	0.34%	−0.66%	−0.12%	0.45%	−0.89%
140	0.35%	−0.07%	0.08%	0.15%	0.49%	−0.90%
150	0.31%	0.29%	−0.03%	0.38%	0.18%	−0.91%

The IPRFGN model is a widespread model based on a conceptual point reactor, which simplifies the real reactor into a point consisting of two operational parameters and 15 characteristic parameters. The KORIGEN solves the whole complex point depletion burnup equation with hundreds of parameters. The code-to-code comparison between the IPRFGN and KORIGEN in HTR-10 validated that the excessively significant parameters are captured. Thus, if the characteristic parameters are correct, the results of the IPRFGN model and the point depletion burnup equation will be similar. Furthermore, validation of other nuclear reactors will be studied in the future.

4.2. Inventories for a Non-Equilibrium Core of HTR-10

Inventories of short-lived fission gas nuclides can be readily calculated for equilibrium and non-equilibrium reactor cores as the characteristic parameters for similar reactor cores tend to be similar. It was observed that only a few operational reactor parameters, including the reactor power and burnup, were needed, as listed in Table 6. The IPRFGN model results are presented in Table 7, which illustrates the non-equilibrium cores of various reactors. The proportion between inventories and reactor power indicates that HTR-10, as a non-equilibrium core, was present in the low burnup region. The inventories of fission gas nuclides in the non-equilibrium HTR-10 core during the experiment time were also determined to have an approximate value of 10^{14} – 10^{16} Bq.

Table 6. Experiments in the primary loop of HTR-10.

Experimental Period	Operational Power (MW)	Average Burnup (GWd/tU)	Number of Fuel Elements
1 December 2004–21 December 2004	9.86	9.35	14,018
5 June 2015–14 June 2015	2.87	29.65	19,327
29 August 2019–31 August 2019	5.93	37.54	19,906

Table 7. Inventories of fission gas nuclides (Bq) for non-equilibrium reactor.

P_{final} (MW/tU)	B (GWd/tU)		
	2.87 MW	5.93 MW	9.86 MW
^{85m}Kr	9.90×10^{14}	1.99×10^{15}	3.68×10^{15}
^{87}Kr	2.06×10^{15}	4.13×10^{15}	7.66×10^{15}
^{88}Kr	3.02×10^{15}	6.07×10^{15}	1.12×10^{16}
^{89}Kr	3.31×10^{15}	6.66×10^{15}	1.24×10^{16}
^{133}Xe	5.70×10^{15}	1.16×10^{16}	2.06×10^{16}
^{133m}Xe	1.64×10^{14}	3.35×10^{14}	5.93×10^{14}
^{135}Xe	3.09×10^{15}	5.07×10^{15}	7.00×10^{15}
^{135m}Xe	7.07×10^{14}	1.44×10^{15}	2.54×10^{15}
^{137}Xe	5.09×10^{15}	1.04×10^{16}	1.83×10^{16}
^{138}Xe	5.36×10^{15}	1.10×10^{16}	1.93×10^{16}
^{85m}Kr	9.90×10^{14}	1.99×10^{15}	3.68×10^{15}
^{87}Kr	2.06×10^{15}	4.13×10^{15}	7.66×10^{15}
^{88}Kr	3.02×10^{15}	6.07×10^{15}	1.12×10^{16}
^{89}Kr	3.31×10^{15}	6.66×10^{15}	1.24×10^{16}
^{133}Xe	5.70×10^{15}	1.16×10^{16}	2.06×10^{16}

5. Conclusions

The novel, simple, and efficient IPRFGN model can be used to interpret and calculate the inventories of short-lived fission gas nuclides. Regardless of the nuclear fission reactor type, the inventories of short-lived fission gas nuclides can be calculated using two steps: (1) determining the point reactor equivalence of a real reactor and (2) calculating solutions for point depletion based on numerous inter-coupled ordinary differential equations.

The IPRFGN model theoretically simplifies the neutron transport module and depletion module, including their coupling. Using the KORIGEN code, any type of fission reactor, such as the equilibrium HTR-10, can be represented by a few characteristic parameters, namely, the neutron flux and the number of fissionable atoms such as ^{235}U , ^{238}U , and ^{239}Pu . Meanwhile, for an individual reactor with a specific loaded fuel, the inventories of short-lived fission gas nuclides are dependent on two crucial condition parameters, namely, the reactor power and the burnup. The IPRFGN model used in this study highlights the physical relationship between the inventories of short-lived fission gas nuclides and the operational parameters of a reactor, and it successfully provided a scientific basis for designing an effective and responsive online core diagnostic system and implementing radiation protections in the primary loop of nuclear reactors.

Based on the results of the equilibrium core of HTR-10, the following conclusions are made in this study: With the exception of ^{135}Xe , all inventories of fission gas nuclides are distributed between the range of 10^{15} – 10^{18} Bq/tU and following descending order of ^{133}Xe , ^{138}Xe , ^{137}Xe , ^{89}Kr , ^{88}Kr , ^{87}Kr , ^{85m}Kr , ^{135m}Xe , and ^{133m}Xe . The inventories of fission gas nuclides excluding ^{135}Xe , i.e., ^{85m}Kr , ^{87}Kr , ^{88}Kr , ^{89}Kr , ^{133}Xe , ^{133m}Xe , ^{135m}Xe , ^{137}Xe , and ^{138}Xe , were proportional to the reactor power. However, the inventory of ^{135}Xe increased with an increase in reactor power and gradually reached equilibrium under a fixed burnup value. All the inventories of fission gas nuclides decreased as the burnup value increased. Several isotopes, such as ^{133}Xe , ^{133m}Xe , ^{137}Xe , and ^{138}Xe , were independent of the burnup in the lower burnup region for a fixed reactor power.

Furthermore, the results for the equilibrium core of HTR-10 were relatively close to those of the values obtained from point depletion burnup programs, such as KORIGEN, with a relative error of <1.0%. Thus, this validates the proposed IPRFGN model used in this study. The inventories of fission gas nuclides in the non-equilibrium HTR-10 core throughout the experiment duration were approximately within the range of 10^{14} – 10^{16} Bq. As predicted by the IPRFGN model, their relationship with the reactor power was consistent.

Finally, as all nuclear fission reactors were found to be reduced to a point reactor, the relationships between the short-lived fission gas nuclide inventories and operational

reaction parameters were similar, and the proposed IPRFGN model can be applied to both equilibrium and non-equilibrium cores of various fission reactors. In the future, the IPRFGN model will be widely used to calculate inventories of fission gas nuclides using a database of characteristic parameters from various reactors.

Supplementary Materials: The following supporting information can be downloaded at: <https://www.mdpi.com/article/10.3390/en16062530/s1>: A justification of most equations in the paper.

Author Contributions: Conceptualization, F.X.; methodology, Y.W.; software, Y.W.; validation, Y.W.; formal analysis, J.C.; investigation, Y.W.; resources, J.C. and F.L.; data curation, Y.W.; writing—original draft preparation, Y.W.; writing—review and editing, F.X. and F.L.; visualization, F.X.; supervision, F.L.; project administration, F.X.; funding acquisition, J.C. All authors have read and agreed to the published version of the manuscript.

Funding: This research was funded by the National Natural Sciences Foundation of China, grant number U2167206, Top-Notch Young Talents Program of China, Young Talent Project of China National Nuclear Corporation, and National S&T Major Project of China, grant number ZX069.

Data Availability Statement: Not applicable.

Acknowledgments: We thank Karl Verfondern and Heinz Nabielek at Research Center Jülich, Jülich, Germany, for helpful discussions.

Conflicts of Interest: The authors declare no conflict of interest.

References

1. Beck, J.M.; Pincock, L.F. *High Temperature Gas-Cooled Reactors Lessons Learned Applicable to the Next Generation Nuclear Plant*; Idaho National Laboratory (INL): Idaho Falls, ID, USA, 2011.
2. Moe, W. *HTGR Mechanistic Source Terms White Paper*; Idaho National Lab. (INL): Idaho Falls, ID, USA, 2010.
3. Kiegiel, K.; Herdzik-Koniecko, I.; Fuks, L.; Zakrzewska-Kołtuniewicz, G. Management of Radioactive Waste from HTGR Reactors including Spent TRISO Fuel—State of the Art. *Energies* **2022**, *15*, 1099. [[CrossRef](#)]
4. Fernández-Arias, P.; Vergara, D.; Orosa, J.A. A Global Review of PWR Nuclear Power Plants. *Appl. Sci.* **2020**, *10*, 4434. [[CrossRef](#)]
5. IAEA. *High Temperature Gas Cooled Reactor Fuels and Materials*; International Atomic Energy Agency: Vienna, Austria, 2010.
6. Nuwayhid, R.; Goddard, A. The potential for gas-cooled reactor development. *Int. J. Energy Res.* **1995**, *19*, 761–789. [[CrossRef](#)]
7. Zhang, Z.; Wu, Z.; Wang, D.; Tong, J. Development Strategy of High Temperature Gas Cooled Reactor in China. *Chin. J. Eng. Sci.* **2019**, *21*, 12–19. [[CrossRef](#)]
8. Sulfredge, C.D.; Lee, R.W. *HPAC Validation against NRC Documentation*; Oak Ridge National Lab. (ORNL): Oak Ridge, TN, USA, 2020.
9. Jeong, H.-D.; Chang, S.-H. Estimation of the fission products, actinides and tritium of HTR-10. *Nucl. Eng. Technol.* **2009**, *41*, 729–738. [[CrossRef](#)]
10. Hanson, D. *A Review of Radionuclide Release from HTGR Cores during Normal Operation, EPRI-1009382*; Electric Power Research Institute: Palo Alto, CA, USA, 2004.
11. Liu, X. *Primary Circuit and Emission Source Term of Nuclear Power Plant*; Beijing Science Press: Beijing, China, 2019.
12. Vela-García, M.; Simola, K. Evaluation of JRC source term methodology using MAAP5 as a fast-running crisis tool for a BWR4 Mark I reactor. *Ann. Nucl. Energy* **2016**, *96*, 446–454. [[CrossRef](#)]
13. Ueta, S.; Aihara, J.; Sakaba, N.; Honda, M.; Furihata, N.; Sawa, K. Fuel performance under continuous high-temperature operation of the HTTR. *J. Nucl. Sci. Technol.* **2014**, *51*, 1345–1354. [[CrossRef](#)]
14. Dangouleme, D.; Inozemtsev, V.; Kamimura, K.; Killeen, J.; Kucuk, A.; Novikov, V.; Onufriev, V.; Tayal, M. IAEA review on fuel failures in water cooled reactors. In Proceedings of the LWR Fuel Performance Meeting/Top Fuel/WRFP 2010, Orlando, FL, USA, 26–29 September 2010; pp. 199–209.
15. Petti, D.A. *A Summary of the Results from the DOE Advanced Gas Reactor (AGR) Fuel Development and Qualification Program*; Idaho National Lab. (INL): Idaho Falls, ID, USA, 2017.
16. Laurie, M.; Fütterer, M.; Appelman, K.; Lapetite, J.-M.; Marmier, A.; Knol, S.; Best, J. On-line fission gas release monitoring system in the High Flux Reactor petten. In Proceedings of the 2013 3rd International Conference on Advancements in Nuclear Instrumentation, Measurement Methods and their Applications (ANIMMA), Marseille, France, 23–27 June 2013; pp. 1–6.
17. Lou, M. *Study on Radiation Monitoring Design of the Primary Coolant Radioactivity in HTR-PM*; Tsinghua University: Beijing, China, 2019.
18. Foudil, Z.; Mohamed, B.; Tahar, Z. Estimating of core inventory, source term and doses results for the NUR research reactor under a hypothetical severe accident. *Prog. Nucl. Energy* **2017**, *100*, 365–372. [[CrossRef](#)]

19. Purwaningsih, A.; Hamzah, A.; Udiyani, P.M.; Setiawan, M.B.; Kuntjoro, S. Estimation of core inventory for PWR 160MWt. In Proceedings of the 4th International Conference on Nuclear Energy Technologies and Sciences (ICoNETS) 2021, Tangerang Selatan, Indonesia, 8 September 2022.
20. Remeikis, V.; Plukis, A.; Juodis, L.; Gudelis, A.; Lukauskas, D.; Druteikienė, R.; Lujanienė, G.; Lukšienė, B.; Plukienė, R.; Duškesas, G. Study of the nuclide inventory of operational radioactive waste for the RBMK-1500 reactor. *Nucl. Eng. Des.* **2009**, *239*, 813–818. [[CrossRef](#)]
21. Rätty, A.; Häkkinen, S.; Kotiluoto, P. Nuclide inventory of FIR 1 TRIGA research reactor fuel. *Ann. Nucl. Energy* **2020**, *141*, 107352. [[CrossRef](#)]
22. Xhonneux, A.; Druska, C.; Struth, S.; Allelein, H.-J. Calculation of the Fission Product Release for the HTR-10 Based on Its Operation History. 2014. Available online: https://inis.iaea.org/search/search.aspx?orig_q=RN:48076850 (accessed on 3 May 2022).
23. Demkowicz, P.; Hunn, J.; Morris, R.; Harp, J.; Winston, P.; Baldwin, C.; Montgomery, F.; Ploger, S.; Rooyen, I.V. *Preliminary Results of Post-Irradiation Examination of the AGR-1 TRISO Fuel Compacts*; Idaho National Laboratory (INL): Idaho Falls, ID, USA, 2012.
24. Li, J.; She, D.; Shi, L.; Liang, J.G. The NUIT code for nuclide inventory calculations. *Ann. Nucl. Energy* **2020**, *148*, 107690. [[CrossRef](#)]
25. Alves, A.M.S.; Heimlich, A.; Lamego, F.; Lapa, C.M.F. The Inventory and Source Term Simulation of the Argonaut Nuclear Reactor Inside a Severe Accident. *Nucl. Technol.* **2020**, *207*, 316–322. [[CrossRef](#)]
26. She, D.; Liu, Y.; Wang, K.; Yu, G.; Forget, B.; Romano, P.K.; Smith, K. Development of burnup methods and capabilities in Monte Carlo code RMC. *Ann. Nucl. Energy* **2013**, *51*, 289–294. [[CrossRef](#)]
27. Duchemin, B.; Nordborg, C. *Decay Heat Calculation an International Nuclear Code Comparison*; Nuclear Energy Agency: Paris, France, 1990.
28. Li, M.; Wang, L.; Yue, W.; Liu, B.; Liu, J.; Liu, Z.; Yan, S.; Yang, X. Metamorphic testing of the NUIT code based on burnup time. *Ann. Nucl. Energy* **2021**, *153*, 108027. [[CrossRef](#)]
29. Ilas, G.; Hiscox, B. *Validation of SCALE 6.2. 4 and ENDF/B-VII. 1 Data Libraries for Nuclide Inventory Analysis in PWR Used Fuel*; Oak Ridge National Lab. (ORNL): Oak Ridge, TN, USA, 2021.
30. Tsilanizara, A.; Huynh, T.D. New feature of DARWIN/PEPIN2 inventory code: Propagation of nuclear data uncertainties to decay heat and nuclide density. *Ann. Nucl. Energy* **2021**, *164*, 108579. [[CrossRef](#)]
31. Castagna, C.; Gilad, E. Study of radionuclide inventory in nuclear fuel under uncertainties in boron concentration using high-fidelity models. *Int. J. Energy Res.* **2022**, *46*, 8007–8019. [[CrossRef](#)]
32. Cui, M.; Wang, Y.; Guo, J.; Zhang, H.; Li, F. Uncertainty Propagation of Fission Product Yields from Uranium and Plutonium in Pebble-Bed HTGR Burnup Calculation. *Energies* **2022**, *15*, 8369. [[CrossRef](#)]
33. Kolobashkin, V.; Rubtsov, P.; Ruzhansky, P.; Sidorenko, V. *Radiation Parameters of Irradiated Nuclear Fuel*; Atomizdat: Moscow, Russia, 1983; Volume 51.
34. Kern, R.; Bonaca, M. Evaluation of Isocheck and Invent Fuel Inventory Computational Models. *Nucl. Appl. Technol.* **1970**, *9*, 796–806. [[CrossRef](#)]
35. Sanz, J.; Cabellos, O.; García-Herranz, N. *ACAB: Inventory Code for Nuclear Applications: User's Manual V. 2008*; National Education Association (NEA): Washington, DC, USA, 2008.
36. Burstall, R.F. *FISPIN—A Computer Code for Nuclide Inventory Calculations*; UKAEA Risley Nuclear Power Development Establishment: Risley, UK, 1979; p. 51.
37. Fleming, M.; Sublet, J.C.; Gilbert, M. FISPACT-II Advanced Nuclear Data Uncertainty Quantification and Propagation Methods. 2017. Available online: https://inis.iaea.org/search/search.aspx?orig_q=RN:53074451 (accessed on 23 December 2021).
38. Tsilanizara, A.; Diop, C.; Nimal, B.; Detoc, M.; Luneville, L.; Chiron, M.; Huynh, T.; Bresard, I.; Eid, M.; Klein, J. DARWIN: An evolution code system for a large range of applications. *J. Nucl. Sci. Technol.* **2000**, *37*, 845–849. [[CrossRef](#)]
39. Sarraf, K. *Docteur de L'Université d'Aix-Marseille*; Aix-Marseille Université: Marseille, France, 2014.
40. Takada, H.; Kosako, K. *Development of the DCHAIN-SP Code for Analyzing Decay and Build-up Characteristics of Spallation Products*; Japan Atomic Energy Research Inst.: Tokyo, Japan, 1999.
41. England, T.R. *CINDER—A One Point Depletion and Fission Product Program*; Westinghouse Electric Corp. Bettis Atomic Power Lab.: West Mifflin, PA, USA, 1962.
42. Bell, M. *ORIGEN: The ORNL Isotope Generation and Depletion Code*; Oak Ridge National Lab.: Oak Ridge, TN, USA, 1973.
43. Croff, A. *ORIGEN2: A Revised and Updated Version of the Oak Ridge Isotope Generation and Depletion Code*; Oak Ridge National Lab.: Oak Ridge, TN, USA, 1980.
44. Hermann, O.; Westfall, R. ORIGEN-S: SCALE system module to calculate fuel depletion, actinide transmutation, fission product buildup and decay, and associated radiation source terms. In *Volume II, Sect. F7 of SCALE: A Modular Code System for Performing Standardized Computer Analyses for Licensing Evaluation, NUREG/CR-0200, Rev*; Oak Ridge National Lab.: Oak Ridge, TN, USA, 1995; Volume 6.
45. Fischer, D.W. *KORIGEN Code*, 1990th ed.; Kernforschungszentrum: Karlsruhe, Germany, 1983.
46. Herber, S.; Allelein, H.; Friege, N.; Kasselmann, S. *First Steps towards a Validation of the New Burnup and Depletion Code TNT*; Deutsches Atomforum e.V.: Berlin, Germany; Kerntechnische Gesellschaft e.V.: Bonn, Germany, 2012.

47. Zhang, Y.; Zhang, Q.; Zhao, Q.; Chi, X.; Zhang, Z.; Huang, K. Development and verification of point-depletion code for PWR. In *International Conference on Nuclear Engineering (ICONE) 2019*; The Japan Society of Mechanical Engineers: Tokyo, Japan, 2019; p. 1681.
48. She, D.; Wang, K.; Yu, G. Development of the point-depletion code DEPTH. *Nucl. Eng. Des.* **2013**, *258*, 235–240. [[CrossRef](#)]
49. Li, J. *Research on the Source Term Analysis Method and Code Development for High Temperature Gas-Cooled Reactor*; Tsinghua University: Beijing, China, 2019.
50. Ma, J.; Huang, H. Development of a new general nuclide inventory analysis code GNIAC. *Ann. Nucl. Energy* **2018**, *115*, 415–422. [[CrossRef](#)]
51. Jiang, S.; Tu, J.; Yang, X.; Gui, N. A review of pebble flow study for pebble bed high temperature gas-cooled reactor. *Exp. Comput. Multiph. Flow* **2019**, *1*, 159–176. [[CrossRef](#)]
52. *Nuclear Reactor Types*; The Institution of Electrical Engineers: London, UK, 2005.
53. Livingstone, S.J. *Development of an On-line Fuel Failure Monitoring System for CANDU Reactors*; Library and Archives Canada: Ottawa, ON, Canada, 2012; Volume 73.
54. Gushev, N.G. *Handbook of Radioactive Characteristics of Fission Products*; Beijing Atomic Energy Press: Beijing, China, 1980.
55. Tuli, J.K. Evaluated nuclear structure data file. *Nucl. Instrum. Methods Phys. Res. Sect. A Accel. Spectrom. Detect. Assoc. Equip.* **1996**, *369*, 506–510. [[CrossRef](#)]
56. Chadwick, M.; Obložinský, P.; Herman, M.; Greene, N.; McKnight, R.; Smith, D.; Young, P.; MacFarlane, R.; Hale, G.; Frankle, S. ENDF/B-VII. 0: Next generation evaluated nuclear data library for nuclear science and technology. *Nucl. Data Sheets* **2006**, *107*, 2931–3060. [[CrossRef](#)]
57. Mills, R.W.; Slingsby, B.M.; Coleman, J.; Collins, R.; Holt, G.; Metelko, C.; Schnellbach, Y. A simple method for estimating the major nuclide fractional fission rates within light water and advanced gas cooled reactors. *Nucl. Eng. Technol.* **2020**, *52*, 2130–2137. [[CrossRef](#)]

Disclaimer/Publisher's Note: The statements, opinions and data contained in all publications are solely those of the individual author(s) and contributor(s) and not of MDPI and/or the editor(s). MDPI and/or the editor(s) disclaim responsibility for any injury to people or property resulting from any ideas, methods, instructions or products referred to in the content.